

Geophysical Research Letters*



RESEARCH LETTER

10.1029/2025GL114906

Key Points:

- We compare isotope-enabled simulations of Dansgaard-Oeschger events from two climate models to a compilation of speleothem oxygen isotope records
- Both models successfully reproduce the signs of the isotopic changes across most of the Northern Hemisphere but generally underestimate their magnitudes
- Remote drivers are more important than local drivers for the regions where the models simulate the most notable isotopic changes

Supporting Information:

Supporting Information may be found in the online version of this article.

Correspondence to:

J. Slattery, johatt11@bas.ac.uk

Citation:

Slattery, J., Sime, L. C., Rehfeld, K., Weitzel, N., Malmierca-Vallet, I., Zhang, X., et al. (2025). A global speleothem-based assessment of spontaneous Dansgaard–Oeschger type oscillations in two isotope-enabled general circulation models. *Geophysical Research Letters*, 52, e2025GL114906. https://doi. org/10.1029/2025GL114906

Received 6 MAY 2025 Accepted 14 SEP 2025

Author Contributions:

Data curation: Irene Malmierca-Vallet, Xu Zhang, Paul J. Valdes Formal analysis: John Slattery, Louise C. Sime, Kira Rehfeld, Nils Weitzel, Francesco Muschitiello Investigation: John Slattery Methodology: John Slattery Supervision: Louise C. Sime, Francesco Muschitiello

Writing - original draft: John Slattery

Conceptualization: John Slattery, Louise

C. Sime, Francesco Muschitiello

© 2025. The Author(s).

This is an open access article under the terms of the Creative Commons

Attribution License, which permits use, distribution and reproduction in any medium, provided the original work is properly cited.

A Global Speleothem-Based Assessment of Spontaneous Dansgaard-Oeschger Type Oscillations in Two Isotope-Enabled General Circulation Models

John Slattery^{1,2}, Louise C. Sime¹, Kira Rehfeld³, Nils Weitzel⁴, Irene Malmierca-Vallet¹, Xu Zhang¹, Paul J. Valdes⁴, and Francesco Muschitiello²

¹Ice Dynamics and Paleoclimate, British Antarctic Survey, Cambridge, UK, ²Department of Geography, University of Cambridge, Cambridge, UK, ³Department of Geosciences, University of Tübingen, Tübingen, Germany, ⁴School of Geographical Sciences, University of Bristol, Bristol, UK

Abstract Several general circulation models have now demonstrated the ability to simulate spontaneous millennial-scale oscillations that resemble Dansgaard–Oeschger (DO) events. It is often unclear how representative of DO events these simulations are, particularly outside of the polar regions. To test this, we directly compare simulated $\delta^{18}O$ changes from two isotope-enabled models to a compilation of 111 speleothem records from 67 caves across the low- and mid-latitudes. We find that both models successfully reproduce the observed pattern of changes in Europe and the Mediterranean, Asia, and Central America. However, they perform less well for Western North America, South America, and Oceania, and the simulated changes are also generally too small in their magnitude. Where the models do reproduce the observed changes, we find evidence that the isotopic variability is influenced by both local and remote drivers, but the remote drivers appear more important.

Plain Language Summary Dansgaard–Oeschger events, also called DO events, are abrupt climate changes that occurred in the Earth's past. Evidence of these abrupt changes can be found in the ratio of different oxygen isotopes contained in cave deposits known as speleothems. We compare the isotope ratios measured in speleothems from different caves around the world to the results of specialized climate models which can directly simulate changes in the numbers of isotopes, to test the accuracy of these models. We find that the models are accurate in some regions, but less so in others, and that the changes they simulate are too small. We also show that the simulated isotope changes occur because of changes to the climate both nearby and further away, with the further away climate changes having the bigger influence.

1. Introduction

During the last glacial period, between approximately 120 ka BP (thousands of years before present) and 10 ka BP, a series of abrupt climate changes, known as Dansgaard–Oeschger (DO) events, occurred (Dansgaard et al., 1993). The trigger of these events may reside in the North Atlantic region (Fohlmeister et al., 2023), and they are prominent in Greenland ice cores (North Greenland Ice Core Project Members, 2004), which show temperature increases of up to 16 K in just a few decades (Kindler et al., 2014) during rapid transitions from cold stadial phases into warm interstadial phases. Speleothem records from across the globe also show shifts in their isotopic signatures that are simultaneous with the Greenland warming (Corrick et al., 2020), indicating that these abrupt changes are global in nature (Buizert et al., 2018; Fohlmeister et al., 2023).

Speleothems form from cave drip-water, the stable oxygen isotope ratio $\delta^{18}O$ of which closely resembles the amount-weighted $\delta^{18}O$ of precipitation (henceforth $\delta^{18}O_p$, Baker et al., 2019). Three key influences on $\delta^{18}O_p$, and so also on cave drip-water $\delta^{18}O$, are the "temperature effect," an observed positive correlation with temperature (Dansgaard, 1964); the "amount effect," an observed negative correlation with precipitation amount (Dansgaard, 1964); and changes in the moisture source (Lachniet, 2009), though some studies are now moving away from the classical "amount effect" and also or instead consider elemental ratios as indicators of wet/dry periods (e.g., Jia et al., 2022). Additional processes occur during the formation of speleothems that can alter the isotopic signal, including temperature-dependent fractionation and site-specific hydrological processes (Lachniet, 2009; Patterson et al., 2024). Although these additional factors can partially obscure the $\delta^{18}O_p$ signal, and thus complicate the interpretation of individual records, speleothems nonetheless represent an excellent source of

SLATTERY ET AL. 1 of 10

Geophysical Research Letters

10.1029/2025GL114906

Writing – review & editing: Louise C. Sime, Kira Rehfeld, Nils Weitzel, Irene Malmierca-Vallet, Xu Zhang, Paul J. Valdes, Francesco Muschitiello information regarding changes to the global hydroclimate (Comas-Bru et al., 2019, 2020) against which we can test the accuracy of model simulations of DO events. This indirectly helps to gauge the appropriate level of confidence regarding projected hydroclimate responses to comparable abrupt changes that are possible in future (DiNezio et al., 2025).

Malmierca-Vallet et al. (2023) showed that an increasing number of general circulation models (GCMs) are now able to simulate spontaneous millennial oscillations that resemble DO events as observed in proxy records (see Malmierca-Vallet et al. (2023) for a full list and thorough review of these models). In evaluating the performance of these models, previous studies have generally focused on evaluating their success in reproducing the observed features of the Greenland temperature and $\delta^{18}O$ records (e.g., Armstrong et al., 2022; Buizert et al., 2024; Sime et al., 2019; Vettoretti et al., 2022; Zhang et al., 2014, 2017, 2021). By contrast, only a limited number of studies have investigated the accuracy of these models across the rest of the globe (e.g., Corrick et al., 2020; Fohlmeister et al., 2023; Izumi et al., 2023), These studies have either only made indirect comparisons between speleothem $\delta^{18}O$ (hereafter $\delta^{18}O_{sp}$) and simulated temperature or precipitation (Corrick et al., 2020; Fohlmeister et al., 2023; Izumi et al., 2023; Zhang et al., 2014), have used simulations in which the oscillations occur due to freshwater forcing (Fohlmeister et al., 2023), or have focused only on a particular region (Dong et al., 2025).

In this study, we conduct the first comprehensive, global comparison between speleothem DO records and spontaneously oscillating, isotope-enabled GCM simulations. This represents a more direct comparison between proxies and models than previous research that considered only simulated temperature or precipitation. We aim to answer the following three questions:

- 1. Do spontaneously oscillating models correctly reproduce the global pattern—that is the signs of the shifts in our six regions—of $\delta^{18}O_{sp}$ changes across DO events?
- 2. Do these models correctly reproduce the magnitude of $\delta^{18}O_{sp}$ changes?
- 3. What are the dominant drivers of the simulated $\delta^{18}O_p$ changes in these models?

2. Materials and Methods

2.1. Proxy Data and Analysis

We take as our benchmark the compilation of abrupt transitions in speleothem $\delta^{18}O_{sp}$ produced by Fohlmeister et al. (2023) using the SISALv2 database (Comas-Bru et al., 2020). This compilation contains 111 speleothem records from 61 cave sites. The 601 individual speleothem transitions in the Fohlmeister et al. (2023) compilation are reasonably evenly distributed across DO events 2–25 (Figure 1), albeit with more recent events slightly overrepresented. Following Fohlmeister et al. (2023), we consider the median value of the interstadial-stadial difference (henceforth notated by Δ) in $\delta^{18}O_{sp}$ across all recorded transitions at each cave site. We group these sites into six geographical regions (see Figure 3), calculating the mean $\Delta\delta^{18}O_{sp}$ across the cave sites in each region to average out some of the variation in the speleothem records due to site-specific cave processes.

To quantify the magnitude of the DO events associated with the speleothem transitions, we calculate the North Greenland Ice Core Project (NGRIP) $\Delta\delta^{18}O$ (North Greenland Ice Core Project Members, 2004) and ΔT (Kindler et al., 2014), consistent with the approach taken by Fohlmeister et al. (2023) to calculate $\Delta\delta^{18}O_{sp}$. The speleothem transitions correspond to DO events with a weighted median NGRIP $\Delta\delta^{18}O$ of 3.4% (Figures 1a and 1d) and a weighted median NGRIP temperature difference ΔT of 8.5 K (Figures 1b and 1e), where the weights are given by the number of speleothem transitions associated with each DO event. If we repeat this separately for each of our six regions, then these values remain relatively consistent, with weighted median NGRIP $\Delta\delta^{18}O$ ranging from 3.4% (5.5% and ΔT from 7.6 to 8.9 K. We can therefore be confident that the Fohlmeister et al. (2023) compilation is a representative benchmark against which to test the spatial pattern of $\delta^{18}O_p$ changes in model simulations, as the speleothem transitions in each region do not appear to be notably biased toward smaller or larger DO events.

2.2. Model Data and Analysis

We investigate two spontaneously oscillating simulations from the isotope-enabled GCMs COSMOS (Dong et al., 2025; Zhang et al., 2021) and HadCM3 (Armstrong et al., 2022; Trombini et al., 2025). Details of these simulations can be found in Supporting Information S1. We use the method of Ditlevsen et al. (2005) to divide the

SLATTERY ET AL. 2 of 10

19448007, 2025, 18, Downloaded from https://agupubs.onli

nelibrary.wiley.com/doi/10.1029/2025GL114906 by British Amarctic Survey, Wiley Online Library on [24/09/2025]. See the Terms and Conditions (https://

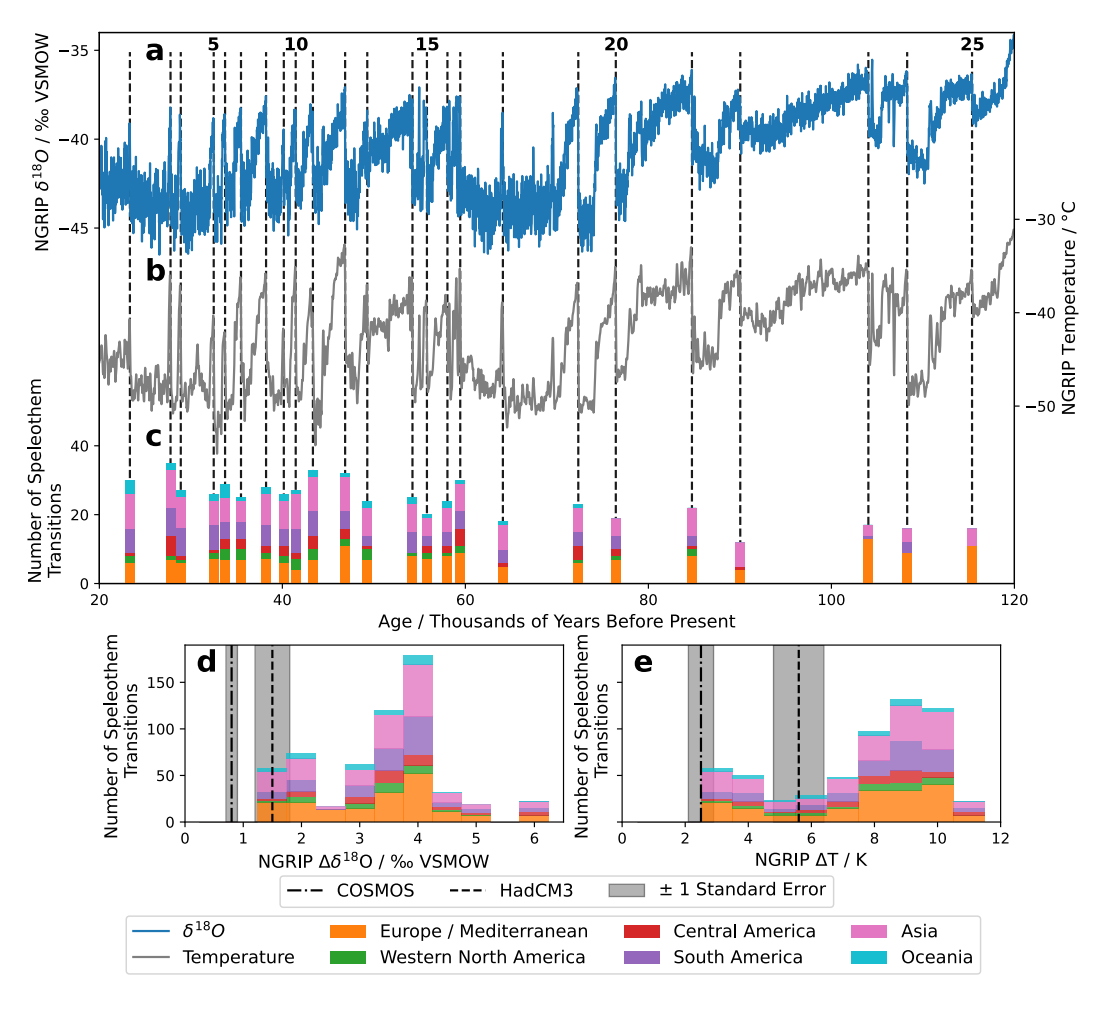


Figure 1. The North Greenland Ice Core Project (NGRIP) $\delta^{18}O$ (a) (North Greenland Ice Core Project Members, 2004) and temperature (b) (Kindler et al., 2014) records from 20 to 120 ka BP, as well as the number of speleothem $\delta^{18}O_{sp}$ transitions in the Fohlmeister et al. (2023) compilation from each of our six regions (as shown in Figure 3) that are associated with each Dansgaard–Oeschger (DO) event (c). DO events 2–25 according to Rasmussen et al. (2014) are marked by dashed lines, with every fifth event labeled above. Also shown are histograms of the NGRIP $\Delta\delta^{18}O$ (d) and ΔT (e) of each DO event, weighted by the number of associated speleothem transitions in each region, and with the simulated $\Delta\delta^{18}O_p$ and ΔT at NGRIP in the two models overlaid.

simulations into stadial and interstadial periods based on the AMOC strength (Figure 2 and Figure S1 in Supporting Information S1). We calculate interstadial-stadial differences in $\delta^{18}O_p$, annual mean temperature T, and annual mean precipitation amount P by subtracting the mean over all stadials from the mean over all interstadials. We use our narrowest and widest definitions to calculate upper- and lower-bound estimates respectively of the interstadial-stadial differences before averaging these two extremes. To calculate the regional mean simulated $\Delta\delta^{18}O_p$, we take the mean over only the grid cells containing speleothem cave sites, weighted by the number of sites in each grid cell.

To allow for direct comparison between the simulated $\Delta\delta^{18}O_p$ and the observed $\Delta\delta^{18}O_{sp}$, we must correct for temperature-dependent fractionation as well as differing standards. Following previous studies (Bühler et al., 2021, 2022; Comas-Bru et al., 2019; Fohlmeister et al., 2023), we convert the speleothem $\Delta\delta^{18}O_{sp}$ values to their drip-water equivalents $\Delta\delta^{18}O_{dw-eq}$ using the equations given by Kim and O'Neil (1997) and Coplen et al. (1983), as well as the simulated ΔT in each model. We verify the robustness of this correction by additionally using a proxy system model (Dee et al., 2015) and demonstrating that the two approaches lead to consistent results (see Supporting Information S1).

SLATTERY ET AL. 3 of 10

19448007, 2025, 18, Downloaded from https://agupubs.onlinelibrary.wiley.com/doi/10.1029/2025GL114906 by British Antarctic Survey, Wiley Online Library on [24/09/2025]. See the Term

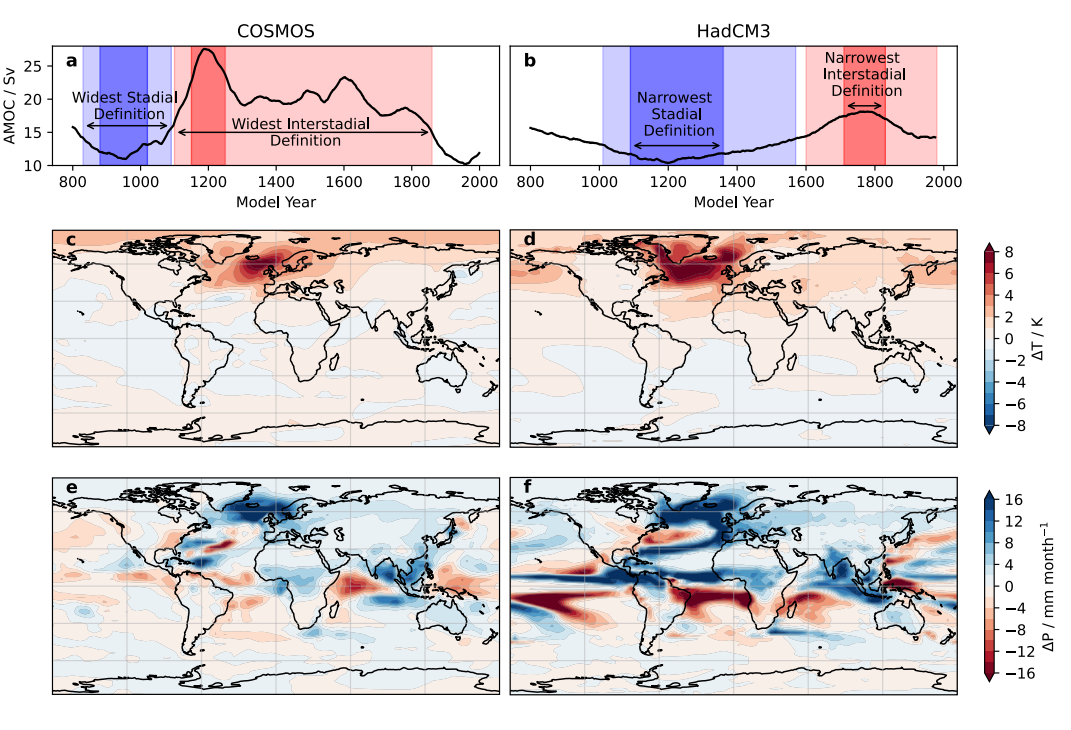


Figure 2. The 50-year running-mean AMOC strength for years 800–2,000 of the (a) COSMOS and (b) HadCM3 simulations. An example stadial (blue) and interstadial (red) period is shaded for each simulation, according to both our widest (pale shading) and narrowest (dark shading) definitions. Also shown are the interstadial-stadial differences (c, d) ΔT and (e, f) ΔP for (c, e) COSMOS and (d, f) HadCM3, (a, b) taking the means of the differences given by our widest and narrowest definitions.

Finally, in investigating the drivers of the variability in simulated $\delta^{18}O_p$ we consider both local and remote factors. For possible local drivers, we focus on precipitation amount P and precipitation-weighted temperature T_p . We separate the variability into interannual and millennial timescales before calculating partial correlations, rather than regular correlations, to alleviate the confounding effect of the correlation between P and T_p (see Supporting Information S1). We decompose the remote drivers into a component from changes to the $\delta^{18}O_{sw}$ of surface seawater in the moisture source regions and a component from changes to the relative contributions of different moisture source regions. We qualitatively assess this second component using changes in precipitation-weighted surface winds.

3. Results

3.1. Changes in AMOC, Temperature, and Precipitation

Our research questions regarding the interstadial-stadial isotopic changes must be considered in the context of the simulated AMOC trajectories as well as the interstadial-stadial differences in temperature and precipitation (Figure 2). The shapes of the AMOC oscillations simulated by COSMOS closely match those of DO events in the Greenland ice core record (Zhang et al., 2021), whereas the oscillations simulated by HadCM3 are too gradual (Armstrong et al., 2022). However, this does not indicate how well these two models may simulate $\Delta \delta^{18}O_p$ globally. Each of the simulations shows a large increase in both temperature and precipitation in the North Atlantic, although they differ in magnitude and in the extent of the affected region. Whilst there is little temperature change across the rest of the world in either model, both show heterogeneous changes in precipitation amount throughout the tropics. In HadCM3, the changes in precipitation over the tropics are indicative of a northward shift in the Inter-Tropical Convergence Zone, however this pattern is not obviously present in COSMOS.

SLATTERY ET AL. 4 of 10

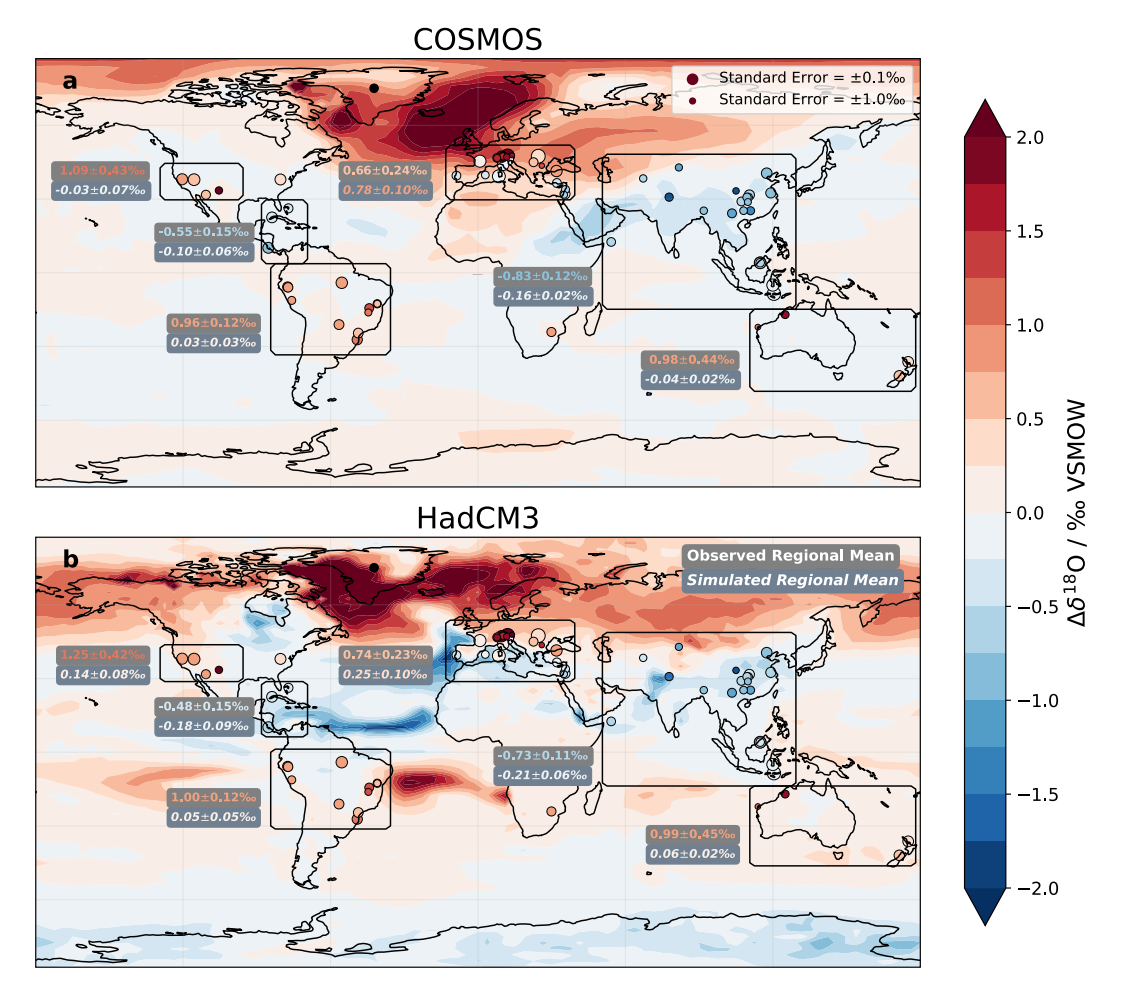


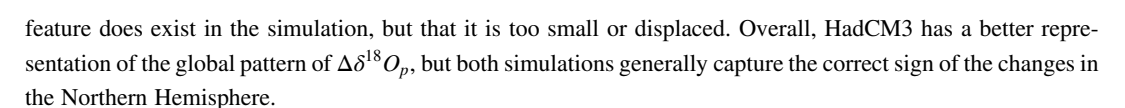
Figure 3. The $\Delta \delta^{18} O_p$ of precipitation in the (a) COSMOS and (b) HadCM3 simulations (contours) along with the median $\Delta \delta^{18} O_{dw-eq}$ at each cave site in the Fohlmeister et al. (2023) speleothem compilation (colored circles). The sizes of these circles indicate the level of uncertainty, accounting for the number and variance of the speleothem transitions at each cave site. Note that the observed values differ slightly between (a) and (b) due to the different simulated temperature changes used to correct for temperature-dependent fractionation in the speleothems. We give the mean observed (upper) and simulated (lower, in italics) values for six regions, where the simulated average is taken over the grid cells containing the cave sites. The given uncertainties for the regional mean values are one standard error. The location of the North Greenland Ice Core Project ice core is also shown with a black dot.

3.2. The Global Pattern of $\delta^{18}O$ Changes

We first consider how successfully the models simulate the observed pattern of changes in the speleothems across the globe by assessing whether the mean simulated $\Delta \delta^{18} O_p$ in each region is of the correct sign. COSMOS has mixed success in this regard (Figure 3a), successfully reproducing the positive mean speleothem $\Delta \delta^{18} O_{dw-eq}$ in the Europe/Mediterranean region (though this positive regional mean masks slightly negative $\Delta \delta^{18} O_{dw-eq}$ values for some coastal sites), as well as the negative mean $\Delta \delta^{18} O_{dw-eq}$ in the Asia and Central America regions. However, it is unable to reproduce the observed changes in Western North America, South America, and Oceania, simulating a regional mean $\Delta \delta^{18} O_p$ that is zero within uncertainty.

Compared to COSMOS, HadCM3 has a better match to the observed pattern of changes (Figure 1b). HadCM3 again correctly reproduces the sign of the mean $\Delta \delta^{18} O_{dw-eq}$ for the Europe/Mediterranean, Asia, and Central America regions, but it additionally reproduces the positive mean $\Delta \delta^{18} O_{dw-eq}$ over Western North America and Oceania. Although HadCM3 again simulates regional mean $\Delta \delta^{18} O_p$ for South America that is zero within uncertainty, it does show large, positive $\Delta \delta^{18} O_p$ over the nearby South Atlantic. This suggests that this observed

SLATTERY ET AL. 5 of 10



3.3. The Magnitude of $\delta^{18}O$ Changes

The two models both simulate smaller changes at NGRIP than the median observed in the NGRIP record (Figure 1). For COSMOS the simulated change in $\delta^{18}O_p$ is $0.8 \pm 0.1\%$ (24% \pm 3% of the median observed change) and the temperature change is 2.6 ± 0.4 K (30% \pm 4% of the observed median), whilst for HadCM3 the change in $\delta^{18}O_p$ is $1.5 \pm 0.3\%$ (40% \pm 10% of the median observed change) and the temperature change is 5.6 ± 0.8 K (67% \pm 9% of the observed median). This suggests that the simulated oscillations in these two models have smaller amplitudes than most DO events as they occurred in the real world, possibly because they are representative only of the successive, smaller DO events that follow non-Heinrich stadials (Zhang et al., 2021) and/or because their sea ice changes are too small (Figure S2 in Supporting Information S1). We must therefore consider $\delta^{18}O_p$ changes in other regions with respect to these small amplitudes at NGRIP.

In COSMOS, the mean simulated $\Delta \delta^{18} O_p$ for our Europe/Mediterranean region is consistent within uncertainties with the mean observed speleothem $\Delta \delta^{18} O_{dw-eq}$, even though this simulation fails to reproduce the negative $\Delta \delta^{18} O_{dw-eq}$ observed around the Mediterranean (Figure 3a). Conversely, the mean simulated $\Delta \delta^{18} O_p$ are too small for Central America (18% \pm 12% of the observed mean) and Asia (19% \pm 4% of the observed mean). The small simulated $\Delta \delta^{18} O_p$ for Central America and Asia are consistent with each other, as well as with the $\Delta \delta^{18} O_p$ simulated at NGRIP, but there is nonetheless an unavoidable inconsistency with the large simulated $\Delta \delta^{18} O_p$ in the Europe/Mediterranean region.

By contrast, in HadCM3 the ratios of simulated $\Delta\delta^{18}O_p$ to observed $\Delta\delta^{18}O_{dw-eq}$ across the Europe/Mediterranean (34% \pm 17%), Central America (37% \pm 22%), and Asia (29% \pm 9%) regions in the Northern Hemisphere all agree within uncertainty. Furthermore, these ratios also all agree with that of simulated $\Delta\delta^{18}O_p$ to observed $\Delta\delta^{18}O$ at NGRIP (40% \pm 10%). This indicates an impressive level of agreement in the magnitude of the simulated changes across disparate regions of the Northern Hemisphere, although Western North America is an exception to this as the ratio of the simulated to observed changes (11% \pm 7%) is too small. The simulated mean in Oceania is also much too small (6% \pm 3% of the observed mean), following the general difficulty that both models have in reproducing the observed changes in the Southern Hemisphere.

3.4. Drivers of $\delta^{18}O_p$ Variability

Next, we examine both the local (temperature and precipitation changes) and remote (moisture source changes) drivers of $\delta^{18}O_p$ variability, starting with the local drivers. The partial correlation between $\delta^{18}O_p$ and T_p at constant $P(\rho_{\delta^{18}O_pT_p,P})$ is generally positive, whilst that between $\delta^{18}O_p$ and P at constant $T_p(\rho_{\delta^{18}O_pP,T_p})$ is generally negative, for both models (Figure 4). These trends respectively reflect the "temperature effect" and the "amount effect" (Dansgaard, 1964). As observed in previous studies that investigated simulations of the last millennium (Bühler et al., 2021, 2022), the temperature effect is generally dominant at high latitudes, whilst the amount effect dominates at low latitudes (Figures 4c and 4f). However, many of our speleothems lie in mid-latitude regions where the dominant influence is unclear; each of temperature and precipitation appear more dominant for subsections of our Asia region, and the two models do not even agree on the sign of $\rho_{\delta^{18}O_pT_p,P}$ here. A broadly similar pattern is seen for millennial variability (Figure S5 in Supporting Information S1). Although this timescale is more directly relevant for understanding the drivers of isotopic changes under DO-like oscillations, the reduction in the effective degrees of freedom due to autocorrelation means that the partial correlations are more uncertain and less statistically significant, particularly for the short HadCM3 simulation. Additionally, at millennial timescales it is more difficult to disentangle the local drivers from the large changes to remote drivers discussed below.

The two models differ in terms of the remote drivers of $\delta^{18}O_p$ variability. Although both models show a positive shift in seawater $\delta^{18}O_{sw}$ in the Arctic and North Atlantic (Figures 4g and 4h), this shift is several times larger in COSMOS (\sim 1.0%) than in HadCM3 (\sim 0.2%). This discrepancy in North Atlantic $\Delta\delta^{18}O_{sw}$ changes explains the difference between the two simulations in the magnitude of the simulated mean $\Delta\delta^{18}O_p$ for the Europe/

SLATTERY ET AL. 6 of 10

19448007, 2025, 18, Downloaded from https://agupubs.onlinelibrary.wiley.com/doi/10.1029/2025GL114906 by British Antarctic Survey, Wiley Online Library on [24/09/2025]. See the Terms

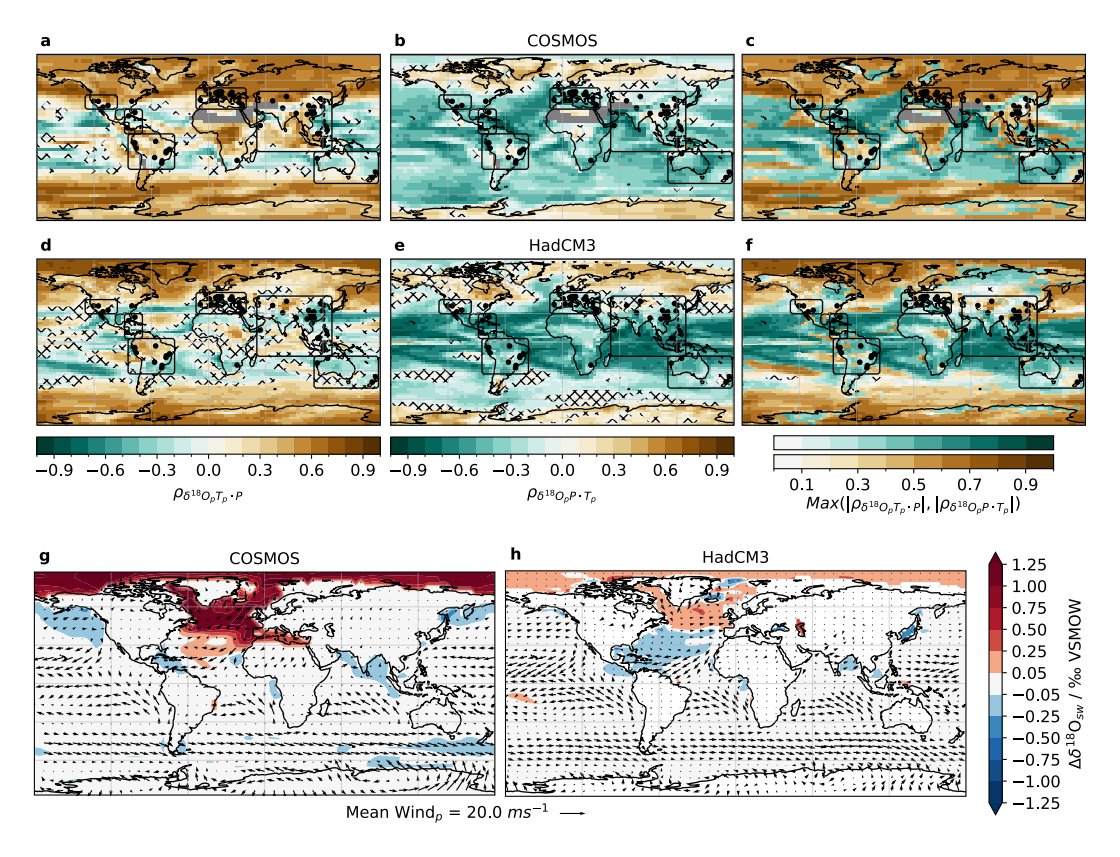


Figure 4. Partial correlations at interannual timescales in (a–c) COSMOS and (d–f) HadCM3. The partial correlation between $\delta^{18}O_p$ and T_p at constant P ($\rho_{\delta^{18}O_pT_p\cdot P}$) is shown in panels (a, d), and that between $\delta^{18}O_p$ and P at constant T_p ($\rho_{\delta^{18}O_pP\cdot T_p}$) is shown in panels (b, e). Panels (c, f) show whichever of these partial correlations is stronger, with green shading where P is dominant, and brown for T_p . Grid cells with partial correlations that are not significant at the 5% level are hatched, whilst those with no precipitation in some years are masked in gray. $\Delta\delta^{18}O_{sw}$ (filled contours) and precipitation-weighted surface wind averaged over both stadials and interstadials (arrows) are also shown for (g) COSMOS and (h) HadCM3.

Mediterranean region. The further southward extent of this feature in COSMOS is also the likely cause of the disagreement between simulation and observation around the Mediterranean (Figure 3). In the Southern Hemisphere, $\delta^{18}O_{sw}$ shows no change in either simulation. A similar pattern is seen in the precipitation-weighted mean surface winds (Figure S4 in Supporting Information S1), in that the only notable changes are in the North Atlantic region.

4. Discussion and Conclusions

We have presented the first comprehensive comparison between speleothem DO records and spontaneously oscillating, isotope-enabled GCM simulations. We have further demonstrated that the Fohlmeister et al. (2023) compilation of abrupt transitions in speleothem $\delta^{18}O_{sp}$ is a representative benchmark data set against which one can assess simulated isotopic changes across DO events over the low-to-mid latitudes of Eurasia and the Americas.

Both COSMOS and HadCM3 accurately capture the observed pattern of the changes across the Europe/Mediterranean, Central America, and Asia regions, whilst HadCM3 also reproduces the observed pattern for Western North America and Oceania. Notably, however, both models entirely fail to simulate the clear isotopic shifts observed in many South American speleothems. Both models also generally underestimate the magnitude of the isotopic changes, as models systematically do for regional, supradecadal variability (Laepple et al., 2023), but the magnitudes of the simulated changes are more consistent across different regions in HadCM3.

Our analysis of the drivers of $\delta^{18}O_{sp}$ changes in the models allows us to comment on possible explanations for the observed isotopic changes in speleothems for those regions in which the models correctly reproduce the signs of the changes. Considering first our Europe/Mediterranean region, the observed positive shifts in speleothem

SLATTERY ET AL. 7 of 10

 $\delta^{18}O_{dw-eq}$ here have previously been suggested as arising either due to local warming through the temperature effect (Corrick et al., 2020), or remotely due to an increase in North Atlantic $\delta^{18}O_{sw}$ (Fohlmeister et al., 2023). Our simulations suggest that both of these drivers play a role, but that the remote change in $\delta^{18}O_{sw}$ of the North Atlantic moisture source is more important.

We next consider Asia, where although $\delta^{18}O_{dw-eq}$ changes in speleothems across DO events have long been considered to indicate changes in Asian Monsoon strength (e.g., Wang et al., 2001, 2008), their precise interpretation has been subject to debate (Cheng et al., 2016). Our analysis lends support to the view that these changes are driven remotely by continent-wide changes in the Asian Monsoon circulation that modulate the moisture sources and transport (He et al., 2021; Tabor et al., 2018). Our simulations show a coherent negative shift in $\delta^{18}O_p$, despite both very small precipitation changes and heterogeneous partial correlations in much of East Asia. This again points toward a dominant role for remote drivers, perhaps linked to the increased precipitation and negative $\Delta\delta^{18}O_{sw}$ which both models simulate in the Bay of Bengal. For Central America, a similar negative shift in seawater $\delta^{18}O_{sw}$ likely also plays a key role.

A further step toward understanding the remote drivers of the observed isotopic changes in would be to quantify the contributions of changes in $\delta^{18}O_{sw}$, as well as in moisture source locations and rainout along moisture pathways. Moisture-tagging experiments using isotope-enabled models would be particularly well suited to addressing this problem, as has recently been demonstrated regarding DO events as observed in Greenland ice cores (Buizert et al., 2024) as well as present day variability in Antarctica (Gao et al., 2024).

Finally, it is also worth considering why these models fail to reproduce the observed changes in Western North America, South America, and Oceania. The simplest explanation is that these regions show no change in either temperature or precipitation (Figure 2). This would imply that these models are missing the teleconnections between the likely origin of DO events in the North Atlantic and their impacts elsewhere around the world.

We have shown that the two models considered in this study have some success in reproducing the observed pattern and magnitude of speleothem $\delta^{18}O$ changes across DO events, justifying their use to understand the processes behind these isotopic shifts. We have also demonstrated evidence for both local and remote drivers of these changes, with the remote drivers more dominant. Based on this study, we suggest the following lines of future research: First, an update to the Fohlmeister et al. (2023) compilation of speleothem transitions using the since-published SISALv3 database (Kaushal et al., 2024) would improve the geographic coverage of the speleothem records and allow for more thorough proxy-model comparisons. Second, further isotope-enabled simulations would allow more models to be tested against speleothems as we have done here. Finally, moisture-tagging experiments would allow for a more comprehensive and quantitative understanding of the impact of remote drivers on the $\delta^{18}O$ changes observed in speleothems.

Data Availability Statement

The compilation of speleothem $\delta^{18}O$ transitions can be reproduced using the code in Fohlmeister et al. (2023). The NGRIP $\delta^{18}O$ record on the GICC05modelext chronology (Wolff et al., 2010) is available from https://www.iceandclimate.nbi.ku.dk/data/2010-11-19_GICC05modelext_for_NGRIP.txt. The NGRIP temperature record is available from the supplement of Kindler et al. (2014) https://doi.org/10.5194/cp-10-887-2014. The code and processed model simulation data required to reproduce the figures in this manuscript are available at https://doi.org/10.5281/zenodo.17037885 (Slattery, 2025).

References

Armstrong, E., Izumi, K., & Valdes, P. (2022). Identifying the mechanisms of DO-scale oscillations in a GCM: A salt oscillator triggered by the Laurentide ice sheet. Climate Dynamics, 60(11–12), 3983–4001. https://doi.org/10.1007/s00382-022-06564-y

Baker, A., Hartmann, A., Duan, W., Hankin, S., Comas-Bru, L., Cuthbert, M. O., et al. (2019). Global analysis reveals climatic controls on the oxygen isotope composition of cave drip water. *Nature Communications*, 10(1), 2984. https://doi.org/10.1038/s41467-019-11027-w

Bühler, J. C., Axelsson, J., Lechleitner, F. A., Fohlmeister, J., LeGrande, A. N., Midhun, M., et al. (2022). Investigating stable oxygen and carbon isotopic variability in speleothem records over the last millennium using multiple isotope-enabled climate models. *Climate of the Past*, 18(7), 1625–1654. https://doi.org/10.5194/cp-18-1625-2022

Bühler, J. C., Roesch, C., Kirschner, M., Sime, L., Holloway, M. D., & Rehfeld, K. (2021). Comparison of the oxygen isotope signatures in speleothem records and iHadCM3 model simulations for the last millennium. Climate of the Past, 17(3), 985–1004. https://doi.org/10.5194/cp-17-985-2021

Acknowledgments

JS was supported by a UK National Environmental Research Council (NERC) C-CLEAR DTP studentship. LCS and XZ were supported by the EU-HE project P2F (HE-101184070). LCS was also supported by the NERC directed projects SWAIS2C (NE/X009386/1) and KANG-GLAC (NE/ V006509/1). XZ was also supported by a National Key Research and Development Projects of China Grant (2023YFF0805 201). KR was supported by the Deutsche Forschungsgemeinschaft (DFG, German Research Foundation) through the STACY project (Project 395588486). NW was supported by the Engineering and Physical Sciences Research Council (EPSRC, Grant EP/Z002591/1). PJV was supported by the NERC Grant NE/S001743/1. FM was supported through a NERC Discovery Science Grant (NE/W006243/1). This work was carried out using the computational facilities of the Advanced Computing Research Centre, University of Bristol. The authors are grateful to three anonymous reviewers for their insightful and constructive feedback

SLATTERY ET AL. 8 of 10



Geophysical Research Letters

- 10.1029/2025GL114906
- Buizert, C., Sigl, M., Severi, M., Markle, B. R., Wettstein, J. J., McConnell, J. R., et al. (2018). Abrupt ice-age shifts in southern westerly winds and Antarctic climate forced from the north. *Nature*, 563(7733), 681–685. https://doi.org/10.1038/s41586-018-0727-5
- Buizert, C., Sowers, T. A., Niezgoda, K., Blunier, T., Gkinis, V., Harlan, M., et al. (2024). The Greenland spatial fingerprint of Dansgaard–Oeschger events in observations and models. *Proceedings of the National Academy of Sciences of the United States of America*, 121(44), e2402637121. https://doi.org/10.1073/pnas.2402637121
- Cheng, H., Edwards, R. L., Sinha, A., Spötl, C., Yi, L., Chen, S., et al. (2016). The Asian monsoon over the past 640,000 years and ice age terminations. *Nature*, 534(7609), 640–646. https://doi.org/10.1038/nature18591
- Comas-Bru, L., Harrison, S. P., Werner, M., Rehfeld, K., Scroxton, N., Veiga-Pires, C., & working group members, S. (2019). Evaluating model outputs using integrated global speleothem records of climate change since the last glacial. *Climate of the Past*, 15(4), 1557–1579. https://doi.org/10.5194/cp-15-1557-2019
- Comas-Bru, L., Rehfeld, K., Roesch, C., Amirnezhad-Mozhdehi, S., Harrison, S. P., Atsawawaranunt, K., et al. (2020). SISALv2: A comprehensive speleothem isotope database with multiple age-depth models. Earth System Science Data, 12(4), 2579–2606. https://doi.org/10.5194/essd-12-2579-2020
- Coplen, T. B., Kendall, C., & Hopple, J. (1983). Comparison of stable isotope reference samples. Nature, 302(5905), 236–238. https://doi.org/10.1038/302236a0
- Corrick, E. C., Drysdale, R. N., Hellstrom, J. C., Capron, E., Rasmussen, S. O., Zhang, X., et al. (2020). Synchronous timing of abrupt climate changes during the last glacial period. Science, 369(6506), 963–969. https://doi.org/10.1126/science.aay5538
- Dansgaard, W. (1964). Stable isotopes in precipitation. Tellus, 16(4), 436. https://doi.org/10.3402/tellusa.v16i4.8993
- Dansgaard, W., Johnsen, S. J., Clausen, H. B., Dahl-Jensen, D., Gundestrup, N. S., Hammer, C. U., et al. (1993). Evidence for general instability of past climate from a 250-kyr ice-core record. *Nature*, 364(6434), 218–220. https://doi.org/10.1038/364218a0
- Dee, S., Emile-Geay, J., Evans, M. N., Allam, A., Steig, E. J., & Thompson, D. (2015). PRYSM: An open-source framework for PRoxY System Modeling, with applications to oxygen-isotope systems. *Journal of Advances in Modeling Earth Systems*, 7(3), 1220–1247. https://doi.org/10.1002/2015MS000447
- DiNezio, P. N., Shanahan, T. M., Sun, T., Sun, C., Wu, X., Lawman, A., et al. (2025). Tropical response to ocean circulation slowdown raises future drought risk. *Nature*, 644(8077), 676–683. https://doi.org/10.1038/s41586-025-09319-x
- Ditlevsen, P. D., Kristensen, M. S., & Andersen, K. K. (2005). The recurrence time of Dansgaard–Oeschger events and limits on the possible periodic component. *Journal of Climate*, 18(14), 2594–2603. https://doi.org/10.1175/JCLI3437.1
- Dong, X., Zhang, X., Zhang, H., Zhang, Y., Rasmussen, S. O., Zhang, R., et al. (2025). Interstadial diversity of East Asian summer monsoon linked to changes of the Northern Westerlies. *Nature Communications*, 16(1), 7765. https://doi.org/10.1038/s41467-025-63057-2
- Fohlmeister, J., Sekhon, N., Columbu, A., Vettoretti, G., Weitzel, N., Rehfeld, K., et al. (2023). Global reorganization of atmospheric circulation during Dansgaard–Oeschger cycles. *Proceedings of the National Academy of Sciences of the United States of America*, 120(36), e2302283120. https://doi.org/10.1073/pnas.2302283120
- Gao, Q., Sime, L. C., McLaren, A. J., Bracegirdle, T. J., Capron, E., Rhodes, R. H., et al. (2024). Evaporative controls on Antarctic precipitation: An ECHAM6 model study using innovative water tracer diagnostics. *The Cryosphere*, 18(2), 683–703. https://doi.org/10.5194/tc-18-683-2024
- He, C., Liu, Z., Otto-Bliesner, B. L., Brady, E., Zhu, C., Tomas, R., et al. (2021). Hydroclimate footprint of pan-Asian monsoon water isotope during the last deglaciation. Science Advances, 7(4), eabe2611. https://doi.org/10.1126/sciadv.abe2611
- Izumi, K., Armstrong, E., & Valdes, P. (2023). Global footprints of Dansgaard-Oeschger oscillations in a GCM. *Quaternary Science Reviews*, 305, 108016. https://doi.org/10.1016/j.quascirev.2023.108016
- Jia, W., Zhang, P., Zhang, L., Li, X., Gao, T., Wang, H., et al. (2022). Highly resolved δ¹³C and trace element ratios of precisely dated stalagmite from northwestern China: Hydroclimate reconstruction during the last two millennia. Quaternary Science Reviews, 291, 107473. https://doi.org/10.1016/j.quascirev.2022.107473
- Kaushal, N., Lechleitner, F. A., Wilhelm, M., Azennoud, K., Bühler, J. C., Braun, K., et al. (2024). SISALv3: A global speleothem stable isotope and trace element database. Earth System Science Data. 16(4), 1933–1963. https://doi.org/10.5194/essd-16-1933-2024
- Kim, S.-T., & O'Neil, J. R. (1997). Equilibrium and nonequilibrium oxygen isotope effects in synthetic carbonates. *Geochimica et Cosmochimica Acta*, 61(16), 3461–3475. https://doi.org/10.1016/S0016-7037(97)00169-5
- Kindler, P., Guillevic, M., Baumgartner, M., Schwander, J., Landais, A., & Leuenberger, M. (2014). Temperature reconstruction from 10 to 120 kyr b2k from the NGRIP ice core. Climate of the Past, 10(2), 887–902. https://doi.org/10.5194/cp-10-887-2014
- Lachniet, M. S. (2009). Climatic and environmental controls on speleothem oxygen-isotope values. Quaternary Science Reviews, 28(5), 412–432. https://doi.org/10.1016/j.quascirev.2008.10.021
- Laepple, T., Ziegler, E., Weitzel, N., Hébert, R., Ellerhoff, B., Schoch, P., et al. (2023). Regional but not global temperature variability underestimated by climate models at supradecadal timescales. *Nature Geoscience*, 16(11), 958–966. https://doi.org/10.1038/s41561-023-01299-9
- Malmierca-Vallet, I., Sime, L. C., & the D-O community members. (2023). Dansgaard-Oeschger events in climate models: Review and baseline marine isotope stage 3 (MIS3) protocol. Climate of the Past, 19(5), 915–942. https://doi.org/10.5194/cp-19-915-2023
- North Greenland Ice Core Project Members. (2004). High-resolution record of Northern Hemisphere climate extending into the last interglacial period. *Nature*, 431(7005), 147–151. https://doi.org/10.1038/nature02805
- Patterson, E. W., Skiba, V., Wolf, A., Griffiths, M. L., McGee, D., Bùi, T. N., et al. (2024). Local hydroclimate alters interpretation of speleothem δ¹⁸O records. *Nature Communications*, 15(1), 9064. https://doi.org/10.1038/s41467-024-53422-y
- Rasmussen, S. O., Bigler, M., Blockley, S. P., Blunier, T., Buchardt, S. L., Clausen, H. B., et al. (2014). A stratigraphic framework for abrupt climatic changes during the last glacial period based on three synchronized Greenland ice-core records: Refining and extending the INTIMATE event stratigraphy. *Quaternary Science Reviews*, 106, 14–28. https://doi.org/10.1016/j.quascirev.2014.09.007
- Sime, L. C., Hopcroft, P. O., & Rhodes, R. H. (2019). Impact of abrupt sea ice loss on Greenland water isotopes during the last glacial period. Proceedings of the National Academy of Sciences of the United States of America, 116(10), 4099–4104. https://doi.org/10.1073/pnas. 1807261116
- Slattery, J. (2025). Code for figures in Slattery et al. (2025) manuscript [Software]. https://doi.org/10.5281/zenodo.17037885
- Tabor, C. R., Otto-Bliesner, B. L., Brady, E. C., Nusbaumer, J., Zhu, J., Erb, M. P., et al. (2018). Interpreting precession-driven 8¹⁸O variability in the South Asian monsoon region. *Journal of Geophysical Research: Atmospheres*, 123(11), 5927–5946. https://doi.org/10.1029/2018JD028424
- Trombini, I., Weitzel, N., Valdes, P. J., Baudouin, J.-P., Armstrong, E., & Rehfeld, K. (2025). Atmospheric and oceanic pathways drive separate modes of Southern Hemisphere climate in simulations of spontaneous Dansgaard-Oeschger-type oscillations. *Geophysical Research Letters*, 52(5), e2024GL111473. https://doi.org/10.1029/2024GL111473
- Vettoretti, G., Ditlevsen, P., Jochum, M., & Rasmussen, S. O. (2022). Atmospheric CO₂ control of spontaneous millennial-scale ice age climate oscillations. *Nature Geoscience*, 15(4), 300–306. https://doi.org/10.1038/s41561-022-00920-7

SLATTERY ET AL. 9 of 10

- Wang, Y., Cheng, H., Edwards, R. L., An, Z. S., Wu, J. Y., Shen, C.-C., & Dorale, J. A. (2001). A high-resolution absolute-dated late Pleistocene monsoon record from Hulu Cave, China. Science, 294(5550), 2345–2348. https://doi.org/10.1126/science.1064618
- Wang, Y., Cheng, H., Edwards, R. L., Kong, X., Shao, X., Chen, S., et al. (2008). Millennial- and orbital-scale changes in the East Asian monsoon over the past 224,000 years. *Nature*, 451(7182), 1090–1093. https://doi.org/10.1038/nature06692
- Wolff, E. W., Chappellaz, J., Blunier, T., Rasmussen, S. O., & Svensson, A. (2010). Millennial-scale variability during the last glacial: The ice core record. *Quaternary Science Reviews*, 29(21), 2828–2838. https://doi.org/10.1016/j.quascirev.2009.10.013
- Zhang, X., Barker, S., Knorr, G., Lohmann, G., Drysdale, R., Sun, Y., et al. (2021). Direct astronomical influence on abrupt climate variability. Nature Geoscience, 14(11), 819–826. https://doi.org/10.1038/s41561-021-00846-6
- Zhang, X., Knorr, G., Lohmann, G., & Barker, S. (2017). Abrupt North Atlantic circulation changes in response to gradual CO₂ forcing in a glacial climate state. *Nature Geoscience*, 10(7), 518–523. https://doi.org/10.1038/ngeo2974
- Zhang, X., Lohmann, G., Knorr, G., & Purcell, C. (2014). Abrupt glacial climate shifts controlled by ice sheet changes. *Nature*, 512(7514), 290–294. https://doi.org/10.1038/nature13592

SLATTERY ET AL. 10 of 10